Letter

Precise approach to determining the ^{3}He neutron incoherent scattering length b_i

H. Lu,[1] O. Holderer,[2] A. Ioffe,[2] S. Pasini,[2] P. Pistel,[3] Z. Salhi,[2] B. M. Goodson,[4] W. M. Snow,[1] and E. Babcock[2,*]

[1]*Indiana University/CEEM, 2401 Milo B. Sampson Lane, Bloomington, Indiana 47408, USA*

[2]*Forschungszentrum Jülich GmbH, Jülich Centre for Neutron Science (JCNS) at Heinz Maier-Leibnitz Zentrum (MLZ), 85747 Garching, Germany*

[3]*Forschungzentrum Jülich GmbH, ZEA-1, 52425 Jülich, Germany*

[4]*School of Chemical and Biomolecular Sciences, Southern Illinois University, Carbondale, Illinois 62901, USA*

(Received 10 March 2023; accepted 25 July 2023; published 11 September 2023)

We report the first results from a new approach for measuring the ^{3}He neutron incoherent scattering length b_i. b_i is directly proportional to the difference $\Delta b = b_+ - b_-$ in the two low-energy s-wave neutron-nucleus scattering amplitudes b_+ and b_-, corresponding to the singlet $J = 0$ and triplet $J = 1$ states of the neutron-^{3}He interaction, respectively. An accurate measurement of b_i can help distinguish among different models of three-nucleon interactions by comparison to *ab initio* nuclear theory calculations. The neutron birefringence caused by Δb results in neutron spin rotation around the nuclear polarization. We measured Δb using polarized neutron spin rotation and the transmission of neutrons through a ^{3}He gas target polarized *in situ* by spin-exchange optical pumping. This brief test measurement performed on the J-NSE Phoenix neutron spin echo spectrometer, yielded $\Delta b = [-5.27 \pm 0.05\ (\text{stat.}) - 0.05\ (\text{syst.})]$ fm. We argue that this method can be improved in precision to resolve the discrepancies between two prior measurements of b_i which are dependent on the polarized absorption cross section σ_p. With absolute ^{3}He polarization measurement via nuclear magnetic resonance (NMR) (in a properly shaped cell) concurrent with accurate neutron transmission measurements, σ_p can be measured to obtain independent values of b_+ and b_-.

DOI: 10.1103/PhysRevC.108.L031001

Precision measurements of the scattering amplitudes in $n + {}^3$He provide important tests for *ab initio* theoretical calculations of the properties of few-nucleon systems. Three-body ($3N$) interactions among nucleons are now estimated to provide about 5% of the total binding energy of stable nuclei [1]. The development of a global model of bound nuclei that can both explain the binding energies of stable nuclei and also make reliable predictions out to the extremes of nuclear stability is a major long-term goal for nuclear physics, with important scientific applications for astrophysics and for our understanding of the process of formation of the heavy elements [2]. Although theoretical models for the possible forms of nuclear three-body forces exist and give a rough estimate for the relative sizes and spin/isospin dependence of three- and higher-body effects compared to two-nucleon forces, more precise experimental data on systems with few nucleons is needed to determine the relative strengths of these forces. The binding energies of ^{3}H, ^{3}He, and ^{4}He are essential data for this purpose in the $A = 4$ system and are measured with high precision. Theoretical calculations of the binding energy of ^{4}He using the Green's function Monte Carlo technique [3] including some using phenomenological three-nucleon interactions [4–7] differ from experiment by 1%. Theoretical analysis also shows that the information on the nuclear three-body force from the binding energy of ^{4}He is not independent of that from three-body bound systems and is mainly sensitive to the spin-independent component of the nuclear three-body force [8–11]. To better constrain the spin-dependent parts of the nuclear three-body force, data are required on the spin-dependent scattering of three- and four-body systems with precision at the subpercent level.

The two best measurements of b_i using neutron spin echo [12] and neutron interferometry [13] are inconsistent based on quoted errors, as are the three measurements of the $n - {}^3$He coherent scattering length b_c using neutron interferometry [14–16]. Different theoretical calculations of b_1 and b_0 then available for comparison employing NN + 3N interactions, such as the standard potential models AV18 + UIX, AV18 + UIX +V3 [17,18], and AV18 + LL2 [19], were also not in agreement. Improved precision on both b_i and b_c can also help distinguish among different models of few-nucleon interactions. Description of the ^{4}He continuum just above the $n + {}^3$He threshold is challenging for existing theory, and changes to existing $3N$ force models are proposed as a possible solution to existing discrepancies. Fortunately several new theoretical techniques have been developed to tackle nuclear four- and five-body systems [20–25] including chiral effective theory [9,26]. Different *ab initio* calculational methods for

*e.babcock@fz-juelich.de

nucleon scattering in $A = 3$ systems deliver internally consistent results [27,28], and the resonating group method (RGM) has been applied in the past to $A = 4$ systems [29,30] thus the prospects for improved theoretical calculations in the $n + {}^3\mathrm{He}$ system are good.

The total free n-nucleus scattering length is given by $a = a' + ia''$, where a' and a'' are real. The imaginary term arises from absorption, which is very large for $n - {}^3\mathrm{He}$. For the forward scattering amplitudes of this work, the bound scattering lengths $b = a(A+1)/A$ are observed, where A is the nucleus to neutron mass ratio. The two s-wave neutron-nucleus scattering amplitudes b_+ and b_-, correspond to the total nucleus plus neutron angular momentum $J = I + s$ and $J = I - s$ scattering channels from a nucleus of spin I and neutron of spin $s = 1/2$. These can be expressed as

$$b = b_c + \frac{2b_i}{\sqrt{I(I+1)}} s \cdot I. \tag{1}$$

The coherent scattering length is thus

$$b_c = \frac{(I+1)b_+ + Ib_-}{(2I+1)} \tag{2}$$

and the incoherent scattering length is

$$b_i = \frac{I\sqrt{I+1}(b_+ - b_-)}{(2I+1)}. \tag{3}$$

The two values $J = 0, 1$ of the total spin for $I = 1/2$ imply $b_+ \equiv b_1$ and $b_- \equiv b_0$ for the triplet and singlet scattering lengths, respectively.

Δb can be measured by observing the precession of the neutron spin as neutrons pass through a polarized nuclear target [31]. Although this phenomenon was initially described [31,32] in terms of a fictitious "pseudomagnetic field" inside the medium, Δb originates from neutron-nucleus scattering. The optical theorem [33] relates the spin dependence of the neutron optical potentials associated with the scattering amplitudes b_+ and b_- to a two-valued neutron index of refraction (n_+, n_-) depending on the relative orientation of the neutron spin and the nuclear polarization:

$$\begin{aligned} n_\pm^2 &= 1 - \frac{4\pi}{k^2} N(b_{\mathrm{coh}} + b_\pm), \\ \Delta n = (n_+ - n_-) &\approx -\frac{2\pi}{k^2} N(b_+ - b_-), \end{aligned} \tag{4}$$

where N is the number of nuclei per unit volume, $k = 2\pi/\lambda$ is the neutron wave number, and the approximation in the second expression is valid in our case as the neutron index of refraction is $\simeq 1$. Δn makes the medium optically birefringent for neutrons so that the two helicity components of the neutron spin accumulate different phases, $kn_\pm d$, in the forward direction as neutrons propagate a distance d through the target. Therefore neutron spins orthogonal to the nuclear polarization direction of the target precess around the nuclear polarization by an angle $\phi^* = k\Delta n d$.

The neutron precession angle ϕ^* from the incoherent scattering length $b_i \propto \Delta b$ of the ${}^3\mathrm{He}$ [12,13] is

$$\phi^* = -\frac{1}{2}\lambda P_3 N d \Delta b = -\frac{2\lambda P_3 N d}{\sqrt{3}} b_i, \tag{5}$$

where P_3 is the ${}^3\mathrm{He}$ polarization, N is the ${}^3\mathrm{He}$ density, and d is the neutron path length through the ${}^3\mathrm{He}$. For nuclei such as ${}^3\mathrm{He}$ which possess a very large spin-dependent component to the neutron cross section, one can determine the constant of proportionality $\lambda P_3 N d$ and write the measured quantity Δb as follows:

$$\Delta b = \frac{2\phi^*}{\lambda P_3 N d} = \frac{\sigma_p}{\lambda_{th.}} \frac{2\phi^*}{\cosh^{-1} R}. \tag{6}$$

Here, R is the ratio of unpolarized neutron transmission of polarized ${}^3\mathrm{He}$, $T(P_3)$, to the transmission of unpolarized ${}^3\mathrm{He}$, $T(0)$, σ_p is the polarized ${}^3\mathrm{He}$ spin dependent neutron absorption cross section, and $\lambda_{th.} = 1.798$ Å is the thermal neutron wavelength used for neutron absorption cross sections. The total $n - {}^3\mathrm{He}$ absorption cross section $\sigma_a = (4\pi/k)b''$ obtained from the imaginary part of b by the optical theorem [33] in terms of the polarization-independent and polarization-dependent terms is

$$\sigma_a = \sigma_{un} \mp P_3 \sigma_p, \tag{7}$$

where the sign convention $\mp$ is for P_3 parallel $(-)$ or antiparallel $(+)$ to the neutron spin. Here, $\sigma_{un} = (5333 \pm 7)$ b is the total unpolarized neutron absorption cross section, and σ_p can be expressed as $\sigma_p = (1 - \sigma_1/\sigma_{un})\sigma_{un}$. Both σ_a and σ_{un} are measured to be proportional to the neutron wavelength λ to high precision [34–36]. For an unpolarized neutron beam of n neutrons with half-spin-up (n^+) and half-spin-down (n^-) neutrons the corresponding transmission of Eq. (7) is

$$T^\pm = \frac{n^\pm}{n} = \frac{1}{2}\exp\left(-(\sigma_{un} \mp P_3\sigma_p)\frac{\lambda N d}{\lambda_{th.}}\right). \tag{8}$$

Thus, the transmission of unpolarized neutrons through polarized ${}^3\mathrm{He}$ is

$$T(P_3) = \exp\left(-\frac{\sigma_{un}}{\lambda_{th.}}\lambda N d\right)\cosh\left(\frac{\sigma_p}{\lambda_{th}}\lambda P_3 N d\right). \tag{9}$$

Since the unpolarized transmission is simply

$$T(0) = \exp\left(-\frac{\sigma_{un}}{\lambda_{th.}}\lambda N d\right) \tag{10}$$

with two neutron transmission measurements giving $R = T(P_3)/T(0)$ one directly experimentally obtains the product $\frac{\sigma_p}{\lambda_{th.}}\lambda P_3 N d$ from $\cosh^{-1} R$, leading to Eq. (6).

One still needs to determine σ_p. If the triplet absorption rate σ_1 were zero, i.e., only absorption in the singlet state σ_0, then $\sigma_p = \sigma_{un}$, where σ_{un} is known to $\simeq 0.1\%$. However the upper bound on σ_p from previous experiments is several percent [35,37] and limits the precision of this technique. There is no reason to expect that σ_1 is zero, as theoretical calculations show [17,18]. Reference [12] used an average of the experimental determinations [35,37] to arrive at a value that can be reinterpreted as $\sigma_1 = 57$ b, conversely Ref. [13] used a combination of theoretical predictions and the measured thermal absorption cross section to estimate $\sigma_1 = 24$ b [13]. For lack of better knowledge of σ_1, we use the latter value in our analysis but also present the result independent of σ_1 as in [13] for comparisons.

${}^3\mathrm{He}$ can also enable a measurement of σ_p. An independent 0.1% measurement of P_3 combined with accurate

measurements of $R(\lambda)$ through an *in situ* polarized ^{3}He sample using the time-of-flight (TOF) method as in Ref. [38] could provide a $\simeq 0.1\%$ accuracy for σ_p, allowing determination of σ_1 to $\approx$5 b accuracy. Atomic physics methods have determined P_3 to high precision [39–42] so this approach should be feasible.

To determine P_3 on a neutron beamline, we propose to use the "self-magnetometry" of a polarized ^{3}He sample in a defined shape, e.g., a long tube parallel or perpendicular to the applied B_0 field. The ^{3}He magnetization $M_3 = \mu_3 P_3 N$ generates a magnetic field of

$$B_3 = \mu_0 M_3 \left(1 - \frac{2}{3}\right) = \mu_0 \frac{M_3}{3} \tag{11}$$

when the tube's axis is parallel to B_0 and

$$B_3 = \mu_0 M_3 \left(\frac{1}{2} - \frac{2}{3}\right) = \mu_0 \frac{-M_3}{6} \tag{12}$$

when the tube's axis is perpendicular to B_0 [39,43]. Here, the first term is the magnetization minus the demagnetization factor and the $-2/3$ term, the field from a spherical volume, arises from the scalar contact term, meaning the ^{3}He spins are nonoverlapping and cannot "see" one another so the self-field must be subtracted [44,45]. The magnetic moment of ^{3}He $\mu_3/h = -16217050$ Hz/T is known to the ppb level [46], and the geometric correction factor for finite length is very well known and is about 2% for a length to diameter ratio $\simeq$5 for the field parallel case [47,48]. At one bar pressure at 25 °C there are 2.43×10^{25} atoms m^3 and the gyromagnetic ratio $\gamma/2\pi = \gamma'$ of ^{3}He is $\gamma_3' = 3.24 \times 10^7$ Hz/T, so the product $f_3 = \mu_0 \mu_3 P_3 N \gamma_3' = 10.6$ Hz for $P_3 = 1$ and $N = 1$ bar. Thus for field-parallel upon an adiabatic fast passage (AFP) reversal of P_3 an NMR frequency shift of

$$\Delta f_3 = 2B_3\gamma_3' = 2\mu_0 \frac{M_3}{3}\gamma_3' = \frac{2}{3}\mu_0\mu_3 P_3 N \gamma_3' \simeq 5\,\text{Hz} \tag{13}$$

will be observed for $P_3 = 0.70$ at 1 bar pressure. λNd of Eq. (9) can be calibrated by unpolarized $T(0,\lambda)$ measurements using the well-known σ_{un} and since one can expect <5 Hz NMR line widths, 0.1% accuracy in P_3 and σ_p should be attainable for normal pressures by signal averaging. No new on-beamline techniques are needed, just a specialized ^{3}He cell. *In situ* polarization of the ^{3}He with AFP and a TOF neutron beamline are preferred.

Since a recent measurement of b_c in $n + {}^4$He using perfect crystal neutron interferometry [49] reached 10^{-3} precision using a technique that can be directly applied to ^{3}He, our ideas to improve b_i are the key additional input needed to confront theory. Therefore we intend to perform a higher precision measurement of $\Delta b/\sigma_p$ and a measurement of σ_p to obtain an absolute value for b_i, which could then also approach a 10^{-3} precision.

We tested a precise method to determine the real part of $\Delta b/\sigma_p$ on the J-NSE Phoenix instrument [50] during an experiment to measure b_i for $n - {}^{129}$Xe and $n - {}^{131}$Xe [51]. Our approach builds on the pioneering work of Zimmer *et al.* [12] by taking advantage of technical improvements in neutron spin echo spectroscopy and by exploiting the improved time stability and performance of polarized ^{3}He gas targets

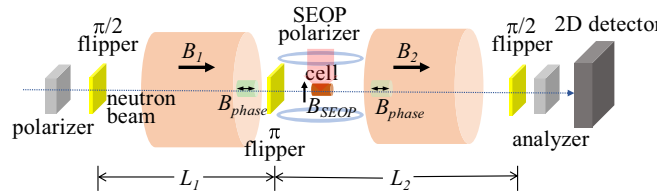

FIG. 1. Schematic of the J-NSE neutron spin echo spectrometer showing field configuration and the SEOP-polarized ^{3}He cell.

created using *in situ* spin-exchange optical pumping (SEOP) [52,53]. Measurements of neutron birefringence in polarized nuclei were originally performed using the Ramsey method of separated oscillatory fields [54,55]. This "pseudomagnetic precession" method [31] uses two oscillating fields before and after a solid-state nuclear-polarized sample to measure the additional phase in the precession caused by it. We employ a variation that also uses orthogonally precessing polarized neutrons moving through a nuclear polarized ^{3}He gas sample but in a neutron spin-echo (NSE) spectrometer [56] to quantify the resulting phase shifts in the neutron precession. NSE is similar to NMR spin echo [57] but the neutron spin is precession-encoded in space for the traveling beam as opposed to in time with static nuclei for NMR spin echo.

In a NSE spectrometer, polarized neutrons are first flipped by $\pi/2$ to induce precession in the orthogonal plane, they then pass through a high-field flight path with an over 1 T m field integral encoding a large number of spin precessions; this step is followed by a π flip reversal of the neutron polarization and then by a second high-field flight path identical to the first to decode the spins. The sample is typically near the middle either before or after the π flipper and the additional precession it creates can be quantified by matching it to the precession in additional phase (compensation) coils placed around the neutron flight path. The NSE method is like the Ramsey technique but the addition of the central π flipper allows the sample-induced phase shift to be quantified by DC phase coils rather than phase-matching of an oscillating RF field. NSE has the benefit that, because the phase coils have field integrals accurate to nT m compared to total instrument field integrals of 1 T m or more, it can encode the spins very precisely and measure very small changes in the neutron precession [50].

A schematic of the NSE spectrometer is shown in Fig. 1. The nuclear spins of the ^{3}He sample were polarized *in situ* using SEOP in the sample area of the NSE spectrometer after the π flipper. The B_{SEOP} field is oriented perpendicular (vertical) to the neutron flight path and main fields B_1 or B_2 of the NSE spectrometer, which are longitudinal (horizontal). The phase coils producing B_{phase} are on either side of the π flipper, the location of which defines the two NSE precession regions L_1 and L_2.

In situ polarization turned out to be advantageous by decoupling time-dependent instrumental drifts from changes in P_3. Using NMR free-induction decay detection, we were able to determine that fractional changes to P_3 were below 0.3%. The *in situ* polarization equipment used also enables on-beam AFP flipping of P_3 during continuous pumping and

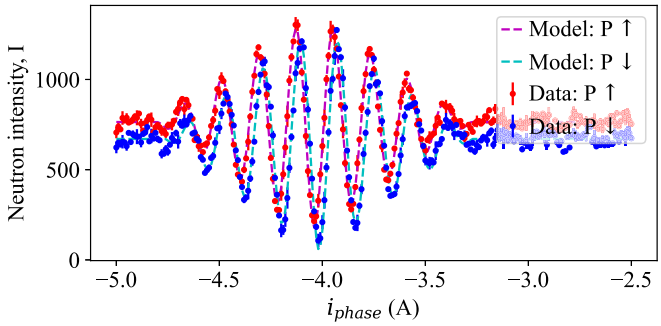

FIG. 2. Spin echo signals from polarized ^{3}He versus the phase coil current for one pixel of the neutron detector. The two profiles correspond to P_3 parallel and antiparallel to B_{SEOP}.

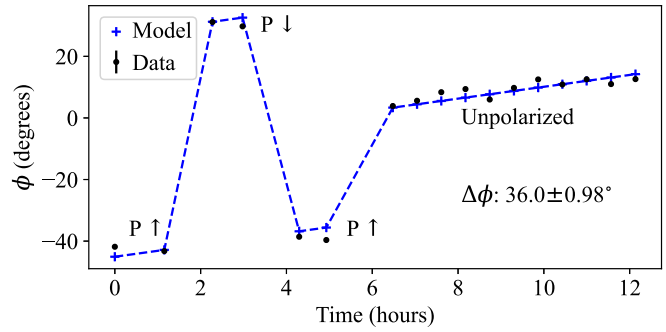

FIG. 3. Phase evolution due to alternating ^{3}He polarizations from one pixel of the NSE detector. The slow drift in ϕ is attributed to the stability of the B_{SEOP} as its location after the π flipper creates an asymmetry in the field integral of L_1 and L_2.

is described in Ref. [53]. The time-dependent phase drifts in the NSE spectrometer are thus fit as a time-dependent background, and the AFP flipping eliminates systematics due to possible non-perfect neutron spin-flips or nonadiabatic transport of the neutron polarization.

A 5 cm diameter cylindrical ^{3}He SEOP cell made of GE180 glass with about 0.4 bar of ^{3}He was used [53]. This cell has rounded ends with a path length of 4.8 cm through its center. In contrast to the neutron polarizer device described in [53,58], here, the vertical magnetic field for SEOP was provided by a set of 70 cm diameter Helmholtz coils for added flexibility and to satisfy space constraints on the J-NSE Phoenix instrument. High-fidelity data were obtained for a 6 cm^2 area, corresponding to 36 detector pixels, through the neutron-illuminated central portion of the cell where the path length is approximately uniform.

A typical NSE scan is made by measuring the amplitude of the neutron polarization vector as the phase-coil is scanned in small steps around the point where the two NSE precession regions are balanced. This action produces a spin echo envelope that shifts in proportion to precession angle ϕ^* of the sample. The J-NSE Phoenix spectrometer employs a position-sensitive detector allowing independent determination of Δb for approximately each 0.5 cm $\times$ 0.5 cm region of the ^{3}He cell, which can then be averaged. This limits corrections that would arise from varying neutron path lengths though the ^{3}He cell. A pair of NSE scans for the two states of the ^{3}He polarization from one such pixel is shown in Fig. 2.

The NSE signal, $I(\Delta i_{\text{phase}})$, is the detected transmitted intensity after the neutron polarization analyzer as a function of the difference in the phase coil currents Δi_{phase}. In the expression

$$I(\Delta i_{\text{phase}}) = I_0\left[1 - p\int d\lambda f(\lambda) cos(\phi_1 - \phi_2)\right], \qquad (14)$$

ϕ_1 and ϕ_2 are the total accumulated precession angles from region L_1 and L_2, respectively, $f(\lambda)$ is the neutron wavelength distribution, p is the loss of contrast of the interference pattern from neutron polarization efficiencies, and I_0 is the transmitted intensity far from the NSE balance point. In addition to the accumulated phase from the field integral of the respective NSE coil B_1 or B_2 and phase coil, ϕ_2 also includes the phase from the field integral of B_{SEOP} and ϕ^* from the sample. The phase coils can be independently tuned to find the center of the NSE where $\phi_1 = \phi_2$.

The current in one phase coil is held constant and the NSE data acquisition system records the position sensitive neutron intensity as the other phase coil is scanned. The neutron wavelength distribution transmitted by the velocity selector is well fit by a triangular function so this form is used to obtain $\int d\lambda f(\lambda)$. The resulting NSE signals were fit for each pixel according to Eq. (14) to obtain ϕ^*, an example of a pair of NSE signals and data fits used for analysis are shown in Fig. 2.

The ^{3}He b_i data reported here were obtained to verify the method for the Xe measurement [51], thus the ^{3}He could only be measured for 12 h. Data were taken in the pattern: two NSE scans with P_3 positive; two scans with P_3 flipped to the negative state; two in the positive state; and six hours of scans with $P_3 = 0$. Although not needed for the determination of b_i, $P_3 = 70.6 \pm 1.6\%$ was determined using R and a value of $[\text{He}] = 0.3556 \pm 0.001$ bar from a separate transmission measurement using neutron TOF on the FIGARO instrument [59]. A graph of the phase versus time for one pixel is shown in Fig. 3. These data were then fit to a step function with a linear time-dependent background to determine the measured shift $\Delta\phi = 2\phi^*$ for $+P_3$ to $-P_3$ for each of the 36 pixels used.

R is determined by taking the weighted average of the mean intensity value of the NSE signal during the NSE scans for the $+P_3$ and $-P_3$ states to determine $T(P)$, and the mean intensity of the unpolarized ^{3}He NSE scans to determine $T(0)$. This process was also performed for each pixel of the NSE scan over our region of interest to account for any variations in d resulting from the cell's shape and alignment in the neutron beam. Using the mean value compensates for the small difference in transmission of the positive versus negative P_3 due to a small residual neutron polarization along B_{SEOP}.

The measured $\Delta\phi$ value has a small correction from the magnetic dipole field of the polarized gas which causes an extra precession signal in the neutron phase that is also proportional to P_3. This effect was discussed in Ref. [12], however that work did not account for the scalar-contact term that one must include for real particles [44,45], which is different than one would expect from the classical result where it is assumed that one can have noninteracting and overlapping point-like particles. For $n - {}^3$He the contact interaction should be 0 for

any reasonable first order approximations. Therefore along their flight path neutrons do not sample the classical field of the individual polarized ^{3}He nuclei inside the cell. The field experienced will consist of the long range dipole fields caused by a nonspherical geometry inside the polarized cell and, since the neutron precession also integrates the field along their entire flight path, the classical field of a polarized (magnetized) volume outside of the cell. For our geometry this would lead to a correction <0.07% and is not yet relevant. Fields experienced by nonzero spin particle beams passing through polarized volumes is of interest for precision measurements and is discussed in the Supplemental Material [60].

The triangular wavelength distribution from the neutron velocity selector leads to a correction because of the wavelength-dependent attenuation of the ^{3}He target. Using the arguments of Ref. [12] this leads to a negligible correction factor of 1.0003 due to the small Nd of the cell used. This correction is not needed for an instrument that uses TOF to determine the transmitted spectrum. Our global detector count rates were 1% or less of the total detector deadtime of 400 ns (e.g., maximum count rate of 2.5 MHz) so deadtime corrections are also negligible.

Using this analysis we obtain $\Delta b = [-5.27 \pm 0.05\ (\text{stat.}) -0.05\ (\text{syst.})]$ fm using the values of $\sigma_{un} = 5333(7)$ barn and an estimated $\sigma_p = \sigma_{un} - \sigma_1 = 5309$ b. From Eq. (5) $\Delta b = 4b_i/\sqrt{3}$ gives the ^{3}He neutron incoherent scattering length. Writing the result independent of σ_p we obtain

$$\frac{\Delta b}{\sigma_p} = (-9.93 \pm 0.09(\text{stat.}) - 0.09(\text{syst.})) \times 10^{-4}\ \frac{\text{fm}}{\text{b}}. \tag{15}$$

This value compares to $\Delta b = [(-10.1929 \pm -.0760) \times 10^{-4}\,\text{fm/b}]\sigma_p$ in Ref. [13] and $\Delta b = [(-10.3628 \pm -.0180) \times 10^{-4}\,\text{fm/b}]\sigma_p$ in Ref. [12]. These preliminary data show we can readily obtain our target of 10^{-3} precision for $\Delta b/\sigma_p$ with a longer measurement. The difference of this preliminary result from previous measurements could be attributed to slow experimental drifts since we were only able to reverse the P_3 once. The cell windows were slightly curved, and a minor shift in the cell position could lead to a one-sided error. Our estimate of the positioning precision of the cell dominate our reported systematic error.

We implemented improvements to the technique of [12] including *in situ* polarization of the ^{3}He gas and the ability to reverse the ^{3}He polarization using AFP. The *in situ* polarization approach decouples the measured ϕ^* from time-dependent drifts that could falsely correlate with P_3, and prevents possible inconsistencies induced by removal and replacement of the ^{3}He cell. The position-sensitive determination of the cross section reduces possible path length errors, which could be further reduced by using a flat-windowed ^{3}He SEOP cell to eliminate variations over time, and the AFP flipping cancels errors from small residual longitudinal neutron polarization. Use of a TOF NSE instrument such as the SNS-NSE [61] will eliminate the neutron velocity selector correction. Since the 0.9% error on our reported value is limited by neutron counting statistics, increasing the measurement time to 1 week (a 14-fold increase) and using a cell with an optimized Nd to minimize error from $\cosh^{-1}(R)$ one could reach a statistical accuracy of <0.1% (or 0.005 fm). Previous work [62] shows that the transmission measurements needed to measure the proportionality factor between ϕ^* and $\Delta b/\sigma_p$ can indeed be conducted with the required precision. With the additional measurement of σ_p to a comparable precision, a total 10^{-3} precision on b_i for ^{3}He can be attained.

H.L. and W.M.S. had support from US National Science Foundation (NSF) Grants No. PHY-1913789 and No. PHY-2209481 and the Indiana University Center for Spacetime Symmetries. H.L. received a short-term grant, 2019 No. 57442045 from DAAD the German Academic Exchange Service. B.M.G. had support from the NSF (CHE-1905341), DoD (W81XWH-15-1-0272, W81XWH2010578), and a Cottrell Scholar SEED Award from Research Corporation for Science Advancement. P. Guthfreund (ILL) and K. Zhernenkov performed a calibration measurement of N (i.e., [He]) on FIGARO [59] aiding this work. We thank G. M. Schrank for discussions and M. Huber for detailed discussions of NIST work on b_i and estimates of σ_1 for ^{3}He [13].

[1] M. C. Atkinson, W. H. Dickhoff, M. Piarulli, A. Rios, and R. B. Wiringa, Phys. Rev. C **102**, 044333 (2020).
[2] C. W. Johnson, K. D. Launey, N. Auerbach, S. Bacca, B. R. Barrett, C. R. Brune, M. A. Caprio, P. Descouvemont, W. H. Dickhoff, C. Elster *et al.*, J. Phys. G **47**, 123001 (2020).
[3] H. Kamada, A. Nogga, W. Glockle, E. Hiyama, M. Kamimura, K. Varga, Y. Suzuki, M. Viviani, A. Kievsky, S. Rosati *et al.*, Phys. Rev. C **64**, 044001 (2001).
[4] R. B. Wiringa, S. C. Pieper, J. Carlson, and V. R. Pandharipande, Phys. Rev. C **62**, 014001 (2000).
[5] A. Nogga, H. Kamada, W. Glockle, and B. R. Barrett, Phys. Rev. C **65**, 054003 (2002).
[6] R. Lazauskas and J. Carbonell, Phys. Rev. C **70**, 044002 (2004).
[7] M. Viviani, A. Kievsky, and S. Rosati, Phys. Rev. C **71**, 024006 (2005).
[8] B. S. Pudliner, V. R. Pandharipande, J. Carlson, and R. B. Wiringa, Phys. Rev. Lett. **74**, 4396 (1995).
[9] R. Machleidt and D. R. Entem, Phys. Rep. **503**, 1 (2011).
[10] J. Carlson, S. Gandolfi, F. Pederiva, S. C. Pieper, R. Schiavilla, K. E. Schmidt, and R. B. Wiringa, Rev. Mod. Phys. **87**, 1067 (2015).
[11] A. Baroni, R. Schiavilla, L. E. Marcucci, L. Girlanda, A. Kievsky, A. Lovato, S. Pastore, M. Piarulli, S. C. Pieper, M. Viviani, and R. B. Wiringa, Phys. Rev. C **98**, 044003 (2018).
[12] O. Zimmer, G. Ehlers, B. Farago, H. Humblot, W. Ketter, and R. Scherm, EPJ Direct **4**, 1 (2002).
[13] M. G. Huber, M. Arif, W. C. Chen, T. R. Gentile, D. S. Hussey, T. C. Black, D. A. Pushin, C. B. Shahi, F. E. Wietfeldt, and L. Yang, Phys. Rev. C **90**, 064004 (2014).

[14] H. Kaiser, H. Rauch, G. Badurek, W. Bauspiess, and U. Bonse, Z. Phys. A **291**, 231 (1979).
[15] P. R. Huffman, D. L. Jacobson, K. Schoen, M. Arif, T. C. Black, W. M. Snow, and S. A. Werner, Phys. Rev. C **70**, 014004 (2004).
[16] W. Ketter, W. Heil, G. Badurek, M. Baron, E. Jericha, R. Loidl, and H. Rauch, Europhys. J A **27**, 243 (2006).
[17] H. M. Hofmann and G. M. Hale, Phys. Rev. C **68**, 021002(R) (2003).
[18] H. M. Hofmann and G. M. Hale, Phys. Rev. C **77**, 044002 (2008).
[19] J. Kirscher, H. W. Griesshammer, D. Shukla, and H. M. Hofmann, Eur. Phys. J. A **44**, 239 (2010).
[20] K. M. Nollett, S. C. Pieper, R. B. Wiringa, J. Carlson, and G. M. Hale, Phys. Rev. Lett. **99**, 022502 (2007).
[21] A. Kievsky, S. Rosati, M. Viviani, L. E. Marcucci, and L. Girlanda, J. Phys. G **35**, 063101 (2008).
[22] P. Navratil, S. Quaglioni, G. Hupin, C. Romero-Redondo, and A. Calci, Phys. Scr. **91**, 053002 (2016).
[23] J. E. Lynn, I. Tews, J. Carlson, S. Gandolfi, A. Gezerlis, K. E. Schmidt, and A. Schwenk, Phys. Rev. Lett. **116**, 062501 (2016).
[24] R. Lazauskas and J. Carbonell, Front. Phys. **7**, 251 (2020).
[25] A. R. Flores and K. M. Nollett, arXiv:2209.00093 [Phys. Rev. C (to be published)].
[26] M. Piarulli and I. Tews, Front. Phys. **7**, 245 (2020).
[27] M. Viviani, A. Deltuva, R. Lazauskas, J. Carbonell, A. C. Fonseca, A. Kievsky, L. E. Marcucci, and S. Rosati, Phys. Rev. C **84**, 054010 (2011).
[28] M. Viviani, A. Deltuva, R. Lazauskas, A. C. Fonseca, A. Kievsky, and L. E. Marcucci, Phys. Rev. C **95**, 034003 (2017).
[29] S. Quaglioni and P. Navrátil, Phys. Rev. Lett. **101**, 092501 (2008).
[30] P. Navrátil, R. Roth, and S. Quaglioni, Phys. Rev. C **82**, 034609 (2010).
[31] V. Baryshevsky and M. Podgoretsky, Zh. Eksp. Teor. Fiz. **47**, 1050 (1964).
[32] A. Abragam and M. Goldman, *Nuclear Magnetism: Order and Disorder* (Clarendon Press, Oxford, 1982).
[33] V. F. Sears, *Neutron Optics: An Introduction to the Theory of Neutron Optical Phenomena and Their Applications* (Oxford University Press, New York, 1989).
[34] J. Als-Nielsen and O. Dietrich, Phys. Rev. **133**, B925 (1964).
[35] S. B. Borzakov, K. Maletski, L. B. Pikelner, M. Stehmpinski, and E. I. Sharapov, Sov. J. Nucl. Phys. **35**, 307 (1982).
[36] C. D. Keith, Z. Chowdhuri, D. R. Rich, W. M. Snow, J. D. Bowman, S. L. Penttilä, D. A. Smith, M. B. Leuschner, V. R. Pomeroy, G. L. Jones, and E. I. Sharapov, Phys. Rev. C **69**, 034005 (2004).
[37] L. Passell and R. I. Schermer, Phys. Rev. **150**, 146 (1966).
[38] T. Chupp, K. Coulter, M. Kandes, M. Sharma, T. Smith, G. L. Jones, W. Chen, T. Gentile, D. Rich, B. Lauss *et al.*, Nucl. Instrum. Methods Phys. Res. A **574**, 500 (2007).
[39] M. V. Romalis and G. D. Cates, Phys. Rev. A **58**, 3004 (1998).
[40] E. Babcock, I. A. Nelson, S. Kadlecek, and T. G. Walker, Phys. Rev. A **71**, 013414 (2005).
[41] P. Nikolaou, A. Coffey, K. Ranta, L. Walkup, B. Gust, M. Barlow, M. Rosen, B. Goodson, and E. Chekmenev, J. Phys. Chem. B **118**, 4809 (2014).
[42] E. Wilms, M. Ebert, W. Heil, and R. Surkau, Nucl. Instrum. Methods Phys. Res. A **401**, 491 (1997).
[43] A. Vlassenbroek, J. Jeener, and P. Broekaert, J. Magn. Reson. A **118**, 234 (1996).
[44] M. V. Romalis, D. Sheng, B. Saam, and T. G. Walker, Phys. Rev. Lett. **113**, 188901 (2014).
[45] M. E. Limes, N. Dural, M. V. Romalis, E. L. Foley, T. W. Kornack, A. Nelson, L. R. Grisham, and J. Vaara, Phys. Rev. A **100**, 010501(R) (2019).
[46] A. Schneider, B. Sikora, S. Dickopf, M. Müller, N. Oreshkina, A. Rischka, I. Valuev, S. Ulmer, J. Walz, Z. Harman *et al.*, Nature (London) **606**, 878 (2022).
[47] D.-X. Chen, E. Pardo, and A. Sanchez, J. Magn. Magn. Mater. **306**, 135 (2006).
[48] R. I. Joseph, J. Appl. Phys. **37**, 4639 (1966).
[49] R. Haun, F. E. Wietfeldt, M. Arif, M. G. Huber, T. C. Black, B. Heacock, D. A. Pushin, and C. B. Shahi, Phys. Rev. Lett. **124**, 012501 (2020).
[50] S. Pasini, O. Holderer, T. Kozielewski, D. Richter, and M. Monkenbusch, Rev. Sci. Instrum. **90**, 043107 (2019).
[51] H. Lu, M. J. Barlow, D. Basler, P. Gutfreund, O. Holderer, A. Ioffe, S. Pasini, P. Pistel, Z. Salhi, K. Zhernenkov, B. M. Goodson, W. M. Snow, and E. Babcock, arXiv:2301.00460.
[52] T. G. Walker and W. Happer, Rev. Mod. Phys. **69**, 629 (1997).
[53] Z. Salhi, E. Babcock, P. Pistel, and A. Ioffe, J. Phys.: Conf. Ser. **528**, 012015 (2014).
[54] N. F. Ramsey, *Molecular Beams* (Oxford University Press, Oxford, 1956).
[55] N. F. Ramsey, Rev. Mod. Phys. **62**, 541 (1990).
[56] F. Mezei, Z. Phys. A **255**, 146 (1972).
[57] E. L. Hahn, Phys. Rev. **80**, 580 (1950).
[58] Z. Salhi, E. Babcock, K. Bingol, K. Bussmann, H. Kammerling, V. Ossovyi, A. Heynen, H. Deng, V. Hutanu, S. Masalovich *et al.*, J. Phys.: Conf. Ser. **1316**, 012009 (2019).
[59] R. A. Campbell, H. P. Wacklin, I. Sutton, R. Cubitt, and G. Fragneto, Eur. Phys. J. Plus **126**, 107 (2011).
[60] See Supplemental Material at http://link.aps.org/supplemental/10.1103/PhysRevC.108.L031001 for a description of the correction due to the magnetic field integral of a polarized particle beam through a polarized target.
[61] M. Ohl, M. Monkenbusch, N. Arend, T. Kozielewski, G. Vehres, C. Tiemann, M. Butzek, H. Soltner, U. Giesen, R. Achten *et al.*, Nucl. Instrum. Methods Phys. Res. A **696**, 85 (2012).
[62] M. M. Musgrave, S. Baessler, S. Balascuta, L. Barron-Palos, D. Blyth, J. D. Bowman, V. Cianciolo, C. Crawford, K. Craycraft, N. Fomin *et al.*, Nucl. Instrum. Methods Phys. Res. A **895**, 19 (2018).